Journal of Alloys and Compounds 773 (2019) 828–837

Contents lists available at ScienceDirect

Journal of Alloys and Compounds

journal homepage: http://www.elsevier.com/locate/jalcom

Tailoring morphology, enhancing magnetization and photocatalytic activity via Cr doping in $Bi_{25}FeO_{40}$

Zhengwei Xiong [a, *], Linhong Cao [b]

[a] Joint Laboratory for Extreme Conditions Matter Properties, Southwest University of Science and Technology and Research Center of Laser Fusion, Southwest University of Science and Technology, Mianyang 621010, China
[b] School of Material Science and Engineering, Southwest University of Science and Technology, Mianyang 621010, China

ARTICLE INFO

Article history:
Received 4 July 2018
Received in revised form
11 September 2018
Accepted 26 September 2018
Available online 26 September 2018

Keywords:
Sillenite
Doping
Band gaps
Photocatalysts

ABSTRACT

The Cr doped $Bi_{25}FeO_{40}$ ($Bi_{25}Fe_{1-x}Cr_xO_{40}$, $x = 0–0.5$) powders were synthesized by a simple hydrothermal process. Effects of the Cr dopant on the crystalline structure, morphologies, optical properties and photocatalytic activities of $Bi_{25}FeO_{40}$ have been investigated. With the increase of Cr concentration, the shape of particles occurs to transformation from regular microcubes ($x = 0$) to microspheres ($x = 0.3$) owing to the lattice expansion. The Fe-O and Cr-O bonds can be coexistence and Fe^{3+} cation could be well replaced by the Cr^{3+} without any secondary phases for the $Bi_{25}Fe_{1-x}Cr_xO_{40}$ ($x \leq 0.3$). Due to the enhanced exchange interaction between Fe2p-O-Cr2p, the decreased optical band gaps and enhancement of magnetization were found. The photo-degradation efficiency for 120 min was significantly enhanced from 43.8% (pure $Bi_{25}FeO_{40}$) to 92.5% ($Bi_{25}Fe_{0.75}Cr_{0.25}O_{40}$), which is nearly 2.1-fold higher than that of undoped $Bi_{25}FeO_{40}$ powders, attributing to cooperative effects of the different morphologies and energy band configurations.

1. Introduction

Semiconductor photocatalytic technology has been considered as an effective approach for the abatement of aqueous pollutants in wastewater and environmental treatment. Among the reported semiconductor-based photocatalysts, TiO_2 bears great hope in solving energy and pollution problems. As we all know, the visible-light occupies ~46% radiation of solar spectra, but TiO_2 can only absorb ultraviolet part of solar light (3–4%). The wide band gap of $E_g = 3.2$ eV results in a low photocatalytic activity under the visible-light irradiation. Thus many researchers try to prepare new photocatalysts with a small E_g matching the visible-light spectrum. According to recent studies, $BiFeO_3$ could also be regarded as a photocatalyst for water splitting and degradation of organic pollutants due to its small band gap (2.2–2.8 eV) [1,2], besides its promising multiferroic applications. Despite its great potential, $BiFeO_3$ suffers from large leakage current owning to the existence of secondary phase during the synthesis and the creation of vacancies such as oxygen or multiple states of Fe [3], which limits the applications of $BiFeO_3$. The site-engineering concept (namely doping) has been widely explored in an effort to reduce the current leakage, improve the ferroelectric and magnetic behaviors [4–6] and enhance the photocatalytic activity in $BiFeO_3$ [7–9] by doping with rare-earth or transition metal either at A-site, or B-site, or A-B-site respectively.

Compared with the $BiFeO_3$ photocatalysts, sillenite-phase $Bi_{25}FeO_{40}$ with a smaller band gap of ~1.8 eV displayed high photocatalytic activity for the degradation of methyl orange, methyl violet and pentachlorophenol under visible-light irradiation [10–12]. Unfortunately, the recent studies show just the opposite results. For example, the $Bi_{25}FeO_{40}$ powders with different morphologies have been prepared using a facile hydrothermal method, and further revealed that the photocatalytic activity could only be enhanced with the aid of some electron scavenging agents such as H_2O_2 molecule [13,14]. This phenomenon is just consistent with the $BiFeO_3$. Luo et al. also reported that, by adding H_2O_2, $BiFeO_3$ nanoparticles could be used as a heterogeneous Fenton-like catalyst, and the enhanced photocatalytic activity was obtained in the $BiFeO_3$-H_2O_2 system [15]. Learning from the ions-doped $BiFeO_3$ with obvious enhancement of photocatalytic ability, we could dope the ions into the $Bi_{25}FeO_{40}$. To our best knowledge, the ions doped $Bi_{25}FeO_{40}$ was rarely investigated.

Additionally, in the doped $BiFeO_3$ catalysts, the transition metal

---

[*] Corresponding author.
E-mail address: zw-xiong@swust.edu.cn (Z. Xiong).

https://doi.org/10.1016/j.jallcom.2018.09.344
0925-8388/

ions with characteristic 3d electrons substituted of Fe^{3+} at B-site, such as Mn, Cr and Ni, forces the optical absorption of the catalysts and supports the separation of photo-generated electron-hole pairs [4,8,16,17]. In a ferroelectric material, the internal dipolar field could induce the band bending at the interfaces and enhance the separation of photon generated charge carriers, further enhancing the photocatalytic activity [7,18]. According to the dipolar interaction between the transition metal, for example Cr-O-Fe or Ni-O-Ti systems [19,20], the internal fields derived from the 3d transitions will behave like photoelectrochemical cells and red-ultraviolet photoluminescence [21,22]. For the A-site doping, Hussain et al. found d-d transition energies in $Bi_{1-x}Sr_xFeO_3$ ($0 < x \leq 0.45$) samples [23]. And for the B-site doping, Vanga et al. also demonstrated that the optical bands and photocatalytic activity could be influenced by the d-d transition between the Fe and doped ions (Cr or Ni) in the $BiFe_{1-x}T_xO_3$ (T = Cr or Ni) systems [4,8]. Based on this, we prepared the Cr ions doped $Bi_{25}FeO_{40}$ by a hydrothermal method, and their variation of structural, surface morphology, band gaps and photocatalytic activity under visible-light irradiation have been presented and discussed.

2. Experimental

2.1. Synthesis of catalyst

Firstly, pure $Bi_{25}FeO_{40}$ powders were fabricated using a simple hydrothermal method. In a typical procedure, a different amount of $Bi(NO_3)_3 \cdot 5H_2O$ (8.1414, 8.1415, 8.1429, 8.1410 and 8.1421 g) and $Fe(NO_3)_3 \cdot 9H_2O$ (0.8073, 0.6459, 0.5397, 0.4649 and 0.4003 g) were suitably mixed in 80 mL of 1 mol/L ethanediol and magnetic stirring for 30 min, forming the different molar ratio of 8:1, 10:1, 12:1, 14:1 and 16:1 between the $Bi(NO_3)_3 \cdot 5H_2O$ and $Fe(NO_3)_3 \cdot 9H_2O$, respectively. Due to the volatility of Bi element, the ratio between the actual amount and theoretical value for the $Bi(NO_3)_3 \cdot 5H_2O$ was set as 1.05:1. According to optimize the molar ratios, the pure phase of $Bi_{25}FeO_{40}$ without any second phases was obtained at the preferable ratio of 12:1 and 14:1, as shown in Fig. 1(a). Then 1 mol/L potassium hydroxide (KOH) solution was slowly added into the solution until PH value about 10 under stirring vigorously. A brown precipitate was formed and then washed with distilled water until PH value about 7. Suspension solution was transferred into a noncorrosive steel reactor with a Teflon liner of 100 mL capability and filled with up to 70% of the total volume. The autoclave was heated at 180 °C for 12 h, and then cooled down to room temperature naturally. The resulting products were washed with deionized water three times, and dried at 70 °C for 6 h.

Based on this, the Cr ions were doped in the $Bi_{25}FeO_{40}$ with different concentration determined by adding the different $Cr(NO_3)_3 \cdot 5H_2O$ contents, which the composition formulae can be signed as $Bi_{25}Fe_{1-x}Cr_xO_{40}$, where the x is in the ranges from x = 0 (pure $Bi_{25}FeO_{40}$) to x = 0.5 ($Bi_{25}Fe_{0.5}Cr_{0.5}O_{40}$).

2.2. Characterization

The crystalline structure of the samples were investigated by X-ray diffraction (XRD) with Cu K_α radiation ($\lambda = 1.5418$ Å). The morphologies of synthesized $Bi_{25}Fe_{1-x}Cr_xO_{40}$ powders were investigated by the scanning electron microscope (SEM), and the chemical compositions were examined by using energy dispersive spectroscopy (EDS) attached with SEM. X-ray photoelectron spectroscopy (XPS) measurements were carried out on analyzing valence states of elements in the materials with a monochromatic Al K_α (1486.8 eV) source. The Fourier transform infrared (FT-IR) spectrum was collected for chemical bonds of the samples at the wavenumbers of 400–1000 cm^{-1}. Diffuse reflectance spectra (DRS) were measured using Jasco UV–Vis spectrometer model V670 in the range of 200–1000 nm. The data obtained from the DRS were converted to absorption spectra using Kulbeka-Munk (K-M) function, further fitting the optical band gaps. Magnetization measurements were performed in a commercial superconducting quantum interference device magnetometer (SQUID) magnetometer (Quantum Design, MPMS XL-5) at room temperature and

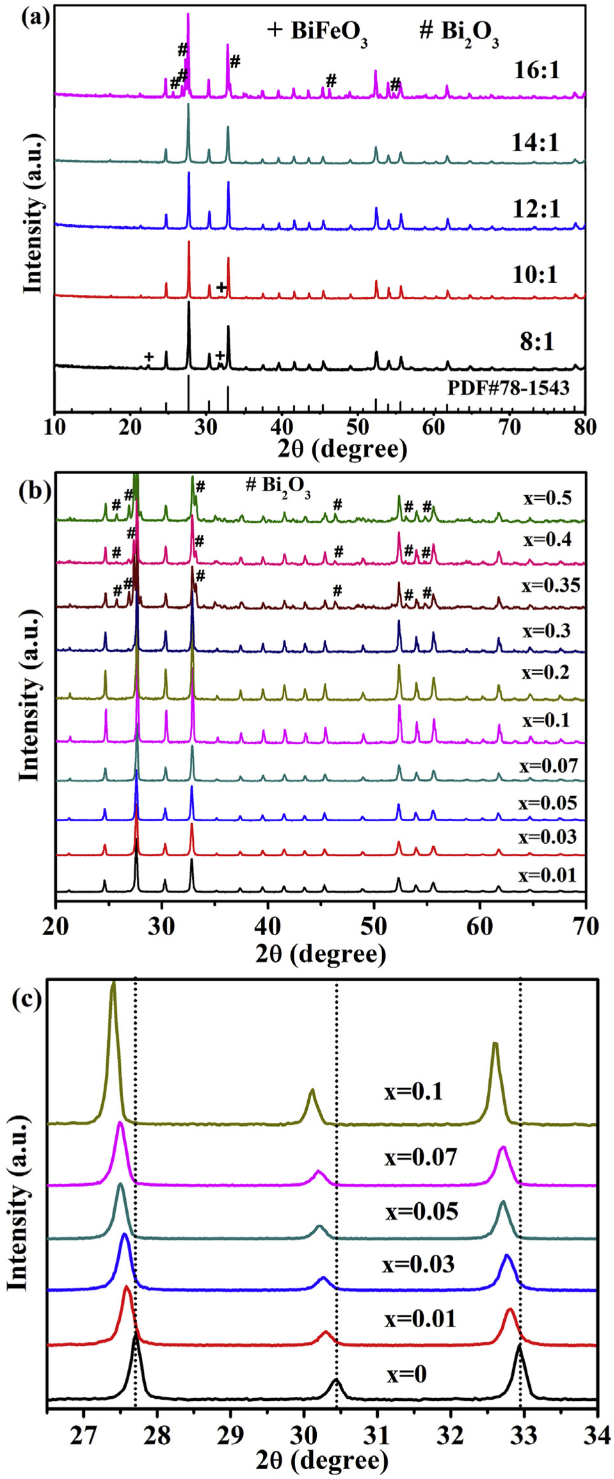

Fig. 1. XRD patterns of as-prepared samples with (a) different R(Bi/Fe), (b) different concentrations of Cr doping on the basic of R(Bi/Fe) = 12:1, (c) expanded view.